

Time-dependent screening of the carrier-phonon and carrier-carrier interactions in nonequilibrium systems

Q. T. Vu and H. Haug

Institut für Theoretische Physik, J.W. Goethe-Universität Frankfurt, Robert-Mayer Str. 8, D 60054 Frankfurt, Germany

(Received 7 February 2000)

For a nonequilibrium electron system in semiconductors the time-dependent screened effective interaction due to longitudinal optical phonon and Coulomb scattering is derived. The polarization is described in terms of a time-dependent random-phase approximation. The nonequilibrium electron propagators are expressed in terms of the single-time density matrix by means of the generalized Kadanoff-Baym approximation. We illustrate the theory for a femtosecond-pulse-excited semiconductor by calculating the resulting two-time-dependent interaction. Using an incomplete Fourier transformation we study the buildup of the phonon-plasmon double resonance in time as a function of the excited carrier density.

I. INTRODUCTION

In an equilibrium electron gas such as occurs, e.g., in heavily doped semiconductors, the longitudinal excitations of the optical phonons and plasmons have similar energies. Indeed, it is well-known that an effective screened interaction that combines the exchange of these two longitudinal collective modes can be given elegantly in the random-phase approximation (RPA), in which the polarization diagram is expressed by a pair of electron propagators (see, e.g., Ref. 1). The poles of the resulting screened effective interaction yield the well-known LO-phonon-plasmon mixed modes. Diagrammatically the effective interaction is determined in this approximation by the graphs of Fig. 1.

In nonequilibrium electron systems, which can be studied most clearly in femtosecond laser pulse excited semiconductors,^{2,3} the theory of the screened Coulomb interaction requires the self-consistent calculation of a two-time-dependent screened Coulomb potential.⁴ The time-dependent RPA polarization bubble is expressed by a pair of two-time-dependent electron propagators, which as a simplification have been expressed in terms of the one-time density matrix. In this so-called generalized Kadanoff-Baym approximation (GKBA) the buildup of the correlation in time is expressed in terms of the retarded and advanced Green functions.⁵ It has been shown that for carrier densities of $10^{17} - 10^{18} \text{ cm}^{-3}$ excited with pulses of duration 10–50 fs the buildup of screening takes place in a time range of a few hundred femtoseconds. The order of buildup time is given by the inverse plasma frequency of the system of optically excited carriers. An attempt to extend the equilibrium Green function theory of the joint treatment of the Coulomb interaction and the interaction with LO phonons for nonequilibrium systems does not seem to be possible at first sight, because of the rather different time structures of the instantaneous bare Coulomb potential and the oscillatory behavior of the phonon propagator. A closer inspection shows, however, that such an extension is possible, starting with a formulation on the Keldysh time contour⁶ for all involved propagators. For the scattering kinetics one needs the lesser and greater parts of the effective interaction $W^<(t, t')$ and $W^>(t, t')$, respec-

tively. It will be shown in this paper that the greater part of the products of three propagators that occur in the diagrammatic equation for the effective interaction potential W (see Fig. 1) can be conveniently evaluated using the Langreth theorem.^{7,3} The resulting equation for the effective two-time-dependent scattering potential $W^>(t, t')$ is simplified again using the GKBA. The electron density matrix and the effective scattering potential are self-consistently evaluated for the example of a femtosecond-pulse-excited two-band semiconductor. The semiconductor Bloch equations for the electron density matrix, which includes the delayed quantum kinetic scattering integrals in terms of the self-consistent GW approximation, are solved together with the equations of the effective scattering potentials $W^<$ and $W^>$. Finally, using an incomplete Fourier transformation, we analyze the buildup of the LO-phonon-plasmon double resonance structure in the resulting complex, time- and frequency-dependent dielectric function of the effective interaction.

II. EFFECTIVE POTENTIAL FOR COMBINED LO-PHONON-COULOMB SCATTERING

In the following we consider a spatially homogeneous nonequilibrium electron system. The exchanged momentum in an interaction process is called \vec{q} . For brevity the vector character is specified only when necessary. Using time arguments—abbreviated as numbers—on the Keldysh contour⁶ that extends from $-\infty$ to the largest time and back to $-\infty$, the effective screened potential $W_q(1,2)$ for the LO-phonon and the Coulomb interactions obeys

$$W_q(1,2) = W_q^0(1,2) + W_q^0(1,3)L_q(3,4)W_q(4,2), \quad (2.1)$$

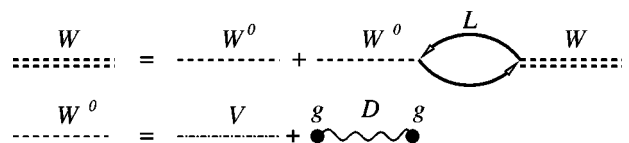


FIG. 1. Graphs for the effective potential W . Here V is the Coulomb potential, D the phonon propagator, L the polarization function, and g the matrix element of the electron-phonon interaction.

where $L_q(1,2)$ is the polarization propagator, which will be approximated by the time-dependent RPA, also called the GG-approximation. The combined interaction potential is

$$W_q^0(1,2) = V_q \delta(1,2) + g_q^2 D_q(1,2) \equiv V_q \delta(1,2) + \mathcal{D}_q(1,2). \quad (2.2)$$

g_q is the Froehlich coupling matrix element

$$g_q^2 = \alpha \frac{4\pi\hbar(\hbar\omega_0)^{3/2}}{(2\mu)^{1/2}q^2\mathcal{V}}. \quad (2.3)$$

Here ω_0 is the LO-phonon frequency and μ is the reduced electron-hole (e - h) mass. The dimensionless polaron coupling constant α is given by

$$\alpha = \frac{e^2}{\hbar} \left(\frac{\mu}{2\hbar\omega_0} \right)^{1/2} \left(\frac{1}{\epsilon_\infty} - \frac{1}{\epsilon_0} \right) \quad (2.4)$$

with the high- and low frequency dielectric constants ϵ_∞ and ϵ_0 , respectively. $D_q(1,2)$ is the free propagator of thermal LO phonons, V_q the bare Coulomb potential. Because the LO phonons are treated explicitly, the dielectric constant in the bare Coulomb interaction is now ϵ_∞ :

$$V_q = \frac{4\pi e^2}{\mathcal{V}\epsilon_\infty q^2}. \quad (2.5)$$

Formally one gets

$$W_q(1,2) = V_q \delta(1,2) + \mathcal{D}_q(1,2) + V_q L_q(1,3) W_q(3,2) + \mathcal{D}_q(1,3) L_q(3,4) W_q(4,2). \quad (2.6)$$

The Langreth theorem^{7,3} allows one to get the real time components efficiently from contour time products. If $C(1,2) = A(1,3)B(3,2)$ on the contour, one finds for real times $C^>(t,t') = A^r(t,t_2)B^>(t_2,t') + A^>(t,t_2)B^a(t_2,t')$, where t_2 has to be integrated from $-\infty$ to $+\infty$. Similarly, if on the contour $D = ABC$, one gets for real times $D^> = A^r B^r C^> + A^r B^> C^a + A^> B^a C^a$, where a matrix structure in the time arguments and integrations over repeated times are assumed. Using the Langreth theorem we get the effective scattering potential for LO-phonon and Coulomb interactions:

$$W_q^> = \mathcal{D}_q^> + V_q(L_q^r W_q^> + L_q^> W_q^a) + \mathcal{D}_q^r L_q^r W_q^> + \mathcal{D}_q^r L_q^> W_q^a + \mathcal{D}_q^> L_q^a W_q^a. \quad (2.7)$$

In this formula V_q is a constant in time. All other quantities depend on two time arguments. The advanced potentials W_q^a can be represented as

$$W_q^a(t_1, t_2) = V_q \delta(t_1 - t_2) + \theta(t_2 - t_1) \times [W_q^<(t_1, t_2) - W_q^>(t_1, t_2)]. \quad (2.8)$$

With the symmetry relations $W_q^<(t_1, t_2)^* = -W_q^<(t_2, t_1)$ and $W_q^>(t_1, t_2) = W_q^<(t_2, t_1)$ the equation for the effective scattering potential $W_q^>(t, t')|_{t \geq t'} = w_q^>(t, t')$ becomes

$$\begin{aligned} w_q^>(t, t') = & \mathcal{D}_q^>(t, t') + V_q^2 L_q^>(t, t') + V_q \left(\int_{-\infty}^t dt_1 L_q^r(t, t_1) W_q^>(t_1, t') + 2 \int_{-\infty}^{t'} dt_1 L_q^>(t, t_1) \text{Re}[W_q^>(t', t_1)] \right. \\ & \left. + \int_{-\infty}^t dt_1 \mathcal{D}_q^r(t, t_1) L_q^>(t_1, t') + \int_{-\infty}^{t'} dt_1 \mathcal{D}_q^>(t, t_1) L_q^a(t_1, t') \right) + \int_{-\infty}^t dt_1 \mathcal{D}_q^r(t, t_1) \int_{-\infty}^{t_1} dt_2 L_q^r(t_1, t_2) W_q^>(t_2, t') \\ & + 2 \int_{-\infty}^t dt_1 \mathcal{D}_q^r(t, t_1) \int_{-\infty}^{t'} dt_2 L_q^>(t_1, t_2) \text{Re}[W_q^>(t', t_2)] + \int_{-\infty}^{t'} dt_1 \mathcal{D}_q^>(t, t_1) \int_{t_1}^{t'} dt_2 L_q^a(t_1, t_2) \text{Re}[W_q^>(t', t_2)]. \end{aligned} \quad (2.9)$$

After some rearrangement in order to get definite time ordering between the times t, t', t_1 , and t_2 , one finds the following closed integral equation for the scattering potential:

$$\begin{aligned} w_q^>(t, t') = & \mathcal{D}_q^>(t, t') + V_q^2 L_q^>(t, t') + 2 \left[V_q \left(\int_{-\infty}^{t'} dt_1 \{ L_q^>(t, t_1) \text{Re}[w_q^>(t', t_1)] - \text{Re}[L_q^>(t, t_1)] w_q^>(t', t_1)^* \} \right. \right. \\ & \left. \left. + \int_{t'}^t dt_1 \text{Re}[L_q^>(t, t_1)] w_q^>(t_1, t') + \int_{t'}^t dt_1 \text{Re}[\mathcal{D}_q^>(t, t_1)] L_q^>(t_1, t') + \int_{-\infty}^{t'} dt_1 \{ \mathcal{D}_q^>(t, t_1) \text{Re}[L_q^>(t', t_1)] \right. \right. \\ & \left. \left. - \text{Re}[\mathcal{D}_q^>(t, t_1)] L_q^>(t', t_1)^* \} \right) + \int_{-\infty}^{t'} dt_1 \text{Re}[\mathcal{D}_q^>(t, t_1)] [M_{1,q}(t', t_1) + M_{5,q}(t', t_1)] + \int_{t'}^t dt_1 \text{Re}[\mathcal{D}_q^>(t, t_1)] \right. \\ & \left. \times [M_{3,q}(t_1, t') + M_{2,q}(t_1, t')] + \int_{-\infty}^{t'} dt_1 \mathcal{D}_q^>(t, t_1) M_{4,q}(t', t_1) \right] \end{aligned} \quad (2.10)$$

with

$$M_{1,q}(t', t_1)|_{t' \geq t_1} = \int_{-\infty}^{t_1} dt_2 \{ L_q^>(t_1, t_2) \text{Re}[w_q^>(t', t_2)] - \text{Re}[L_q^>(t_1, t_2)] w_q^>(t', t_2)^* \},$$

$$\begin{aligned}
M_{2,q}(t_1, t')|_{t_1 \geq t'} &= \int_{-\infty}^{t'} dt_2 \{L_q^>(t_1, t_2) \text{Re}[w_q^>(t', t_2)], -\text{Re}[L_q^>(t_1, t_2)]w_q^>(t', t_2)^*\}, \\
M_{3,q}(t_1, t')|_{t_1 \geq t'} &= \int_{t'}^{t_1} dt_2 \text{Re}[L_q^>(t_1, t_2)]w_q^>(t_2, t'), \\
M_{4,q}(t', t_1)|_{t' \geq t_1} &= \int_{t_1}^{t'} dt_2 \text{Re}[L_q^>(t_2, t_1)]\text{Re}[w_q^>(t', t_2)], \\
M_{5,q}(t', t_1)|_{t' \geq t_1} &= \int_{t_1}^{t'} dt_2 L_q^>(t_2, t_1)^* \text{Re}[w_q^>(t', t_2)]. \tag{2.11}
\end{aligned}$$

For the evaluation of this integral equation, we use the time-dependent RPA polarization function

$$L_q(1,2) = -2i\hbar \sum_k G_{\vec{k}}(1,2)G_{\vec{k}-\vec{q}}(2,1). \tag{2.12}$$

In the scattering components of the polarization function, the two-time electron propagators will be expressed in terms of the one-time density matrix and the retarded and advanced Green functions. This so-called generalized Kadanoff-Baym approximation⁵ is

$$G_q^>(t, t') = \mp [G_q^r(t, t')\rho_q^<(t') - \rho_q^>(t)G_q^a(t, t')], \tag{2.13}$$

where $\rho_q^<(t) = \langle a_q^\dagger(t)a_q(t) \rangle \equiv \rho_q(t)$ and $\rho_q^>(t) = \langle a_q(t)a_q^\dagger(t) \rangle = 1 - \rho_q(t)$. It has been shown for the example of LO-phonon scattering by direct numerical calculation of the two-time propagators that in semiconductors with relatively large dielectric constants, i.e., weak interactions, the GKBA yields extremely good results.⁸ Note that the GKBA is exact for equal times, and thus its validity for short time intervals is particularly good. For the retarded and advanced Green functions we will use the following approximation scheme. First, the unitary time development under the time-dependent mean-field Hamiltonian will be calculated self-consistently.⁹ The decay of these functions will be described by a hyperbolic secant law and not by a simple exponential decay law. The hyperbolic secant connects a Gaussian decay for small times with an exponential one for larger times.^{10,11} This decay approximates the actual decay very well¹¹ qualitatively on the femtosecond time scale. These self-consistently determined retarded (and advanced) Green functions take the form

$$\begin{aligned}
G_{\vec{k}}^r(t_1, t_2) &= -i\Theta(t_1 - t_2) \\
&\times [U_{\vec{k}}(t_1)U_{\vec{k}}(t_2)^+] \frac{1}{\cosh^\alpha[\omega_0(t_1 - t_2)]}, \tag{2.14}
\end{aligned}$$

where the unitary time development is determined by

$$i\hbar \frac{dU_{\vec{k}}(t)}{dt} = H_{\vec{k}}^{MF}(t)U_{\vec{k}}(t) \tag{2.15}$$

with the initial condition $U_{\vec{k}}(t=-\infty) = 1$. The mean-field Hamilton operator is $H^{MF} = H_0 + \Sigma^{MF}(t)$, where H_0 is the Hamiltonian of the free particles interacting with a coherent light field and $\Sigma^{MF}(t)$ is the mean-field self-energy. For the example of a pulse-excited semiconductor, it contains the Coulomb exchange energies and the dipole interaction with the laser field. Both terms contain the electron density matrix again. Therefore Eq. (2.10) for the effective screened interaction and the equation for the retarded Green function both contain the electron density matrix. The system of equations has thus to be closed by the equation of motion for the electron density matrix containing both the mean-field development and the dissipative quantum kinetics in terms of the scattering self-energies in the GW approximation, where W is again the effective screened interaction potential introduced above.

III. CALCULATION OF THE TIME-DEPENDENT EFFECTIVE INTERACTION FOR A FEMTOSECOND-PULSE-EXCITED SEMICONDUCTOR

Femtosecond pulses in the optical range are presently as short as 5 fs.¹² This time is shorter than the inverse frequency of LO-phonon oscillations and the inverse plasma frequency for typical excitation densities of $10^{17} - 10^{18} \text{ cm}^{-3}$ assuming resonant band-to-band excitation. Therefore femtosecond semiconductor spectroscopy is ideally suited to examine the quantum kinetic regime of phonon and Coulomb scattering including the buildup of screening of the effective interaction. As mentioned above, the equations for the effective scattering potential $W^>(t, t')$ and for the retarded Green function $G^r(t, t')$ have to be closed by an equation of motion for the electron density matrix $\rho(t)$ in which the dissipative quantum kinetic terms are given by the scattering self-energy $\Sigma^>(t, t')$, which will be taken in the so-called GW approximation. In this approximation vertex corrections are neglected and the self-energy is given in terms of the effective potential in the form

$$\Sigma_k^>(t, t') = i\hbar \sum_q W_q^>(t, t')G_{k+q}^<-(t', t), \tag{3.1}$$

where again the GKBA is used to express the electron propagators in terms of the electron density matrix. The simplest vertex correction with two crossed potential lines leads to-

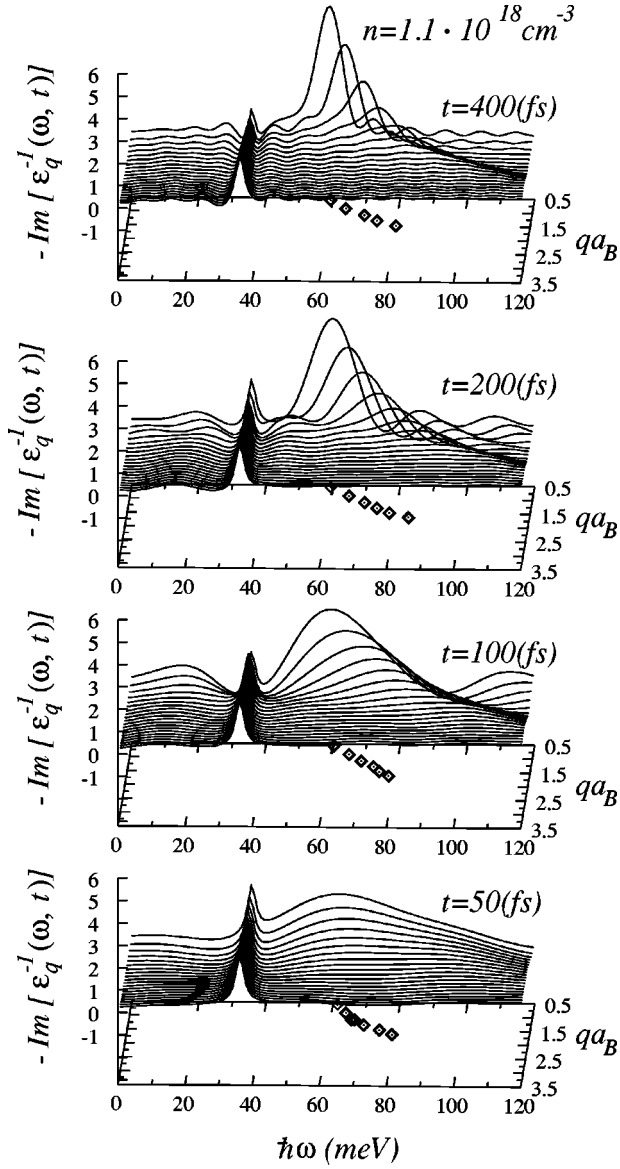


FIG. 2. Negative imaginary part of the inverse dielectric function versus frequency and wave number in units of the exciton Bohr radius a_B for the times $t = 50, 100, 200, 400$ fs after a 11 fs pulse that excites 1.1×10^{18} $e-h$ pairs per cm^3 . The projection of the plasmon resonance into the ω - q plane is indicated by symbols.

gether with Eq. (3.1) to the second Born approximation. In nonequilibrium theory this vertex correction contains two additional time integrations compared to Eq. (3.1). In the femtosecond regime these integrations over short time intervals reduce the contribution of this vertex correction strongly compared to Eq. (3.1). In a two-band semiconductor where the optical transitions take place between the valence band and the conduction band, all particle Green functions, the polarization, the unitary time development matrix, and the density matrix are 2×2 matrices in the band index. For a laser-pulse-excited semiconductor the density matrix equation takes the form

$$\frac{\partial}{\partial t} \rho_{\vec{k}}(t) = \frac{\partial}{\partial t} \rho_{\vec{k}}(t) \Big|_{\text{coh}} + \frac{\partial}{\partial t} \rho_{\vec{k}}(t) \Big|_{\text{scatt}}, \quad (3.2)$$

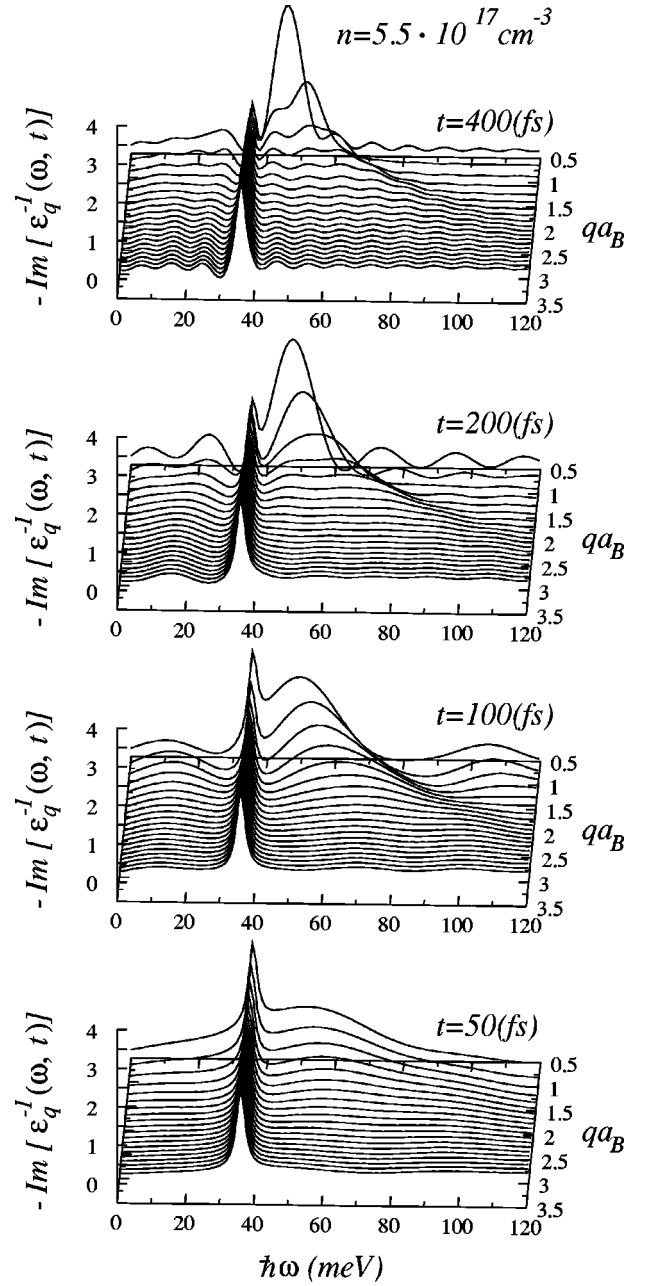


FIG. 3. Negative imaginary part of the inverse dielectric function versus frequency and wave number in units of the exciton Bohr radius a_B for the times $t = 50, 100, 200, 400$ fs after an 11 fs pulse that excites 5.5×10^{17} $e-h$ pairs per cm^3 .

The coherent part of the equation is the so-called semiconductor Bloch equation

$$i\hbar \frac{\partial}{\partial t} \rho_{\vec{k}}(t) \Big|_{\text{coh}} = [H_0 + \Sigma^{MF}(t)]\rho(t) - \rho(t)[H_0 + \Sigma^{MF}(t)], \quad (3.3)$$

where H_0 is the free-particle Hamiltonian interacting with a coherent laser field $E(t)$,

$$H_0 = \begin{pmatrix} E_g + \frac{\hbar^2 k^2}{2m_e} & -\frac{1}{2}dE(t) \\ -\frac{1}{2}dE(t) & -\frac{\hbar^2 k^2}{2m_h} \end{pmatrix}, \quad (3.4)$$

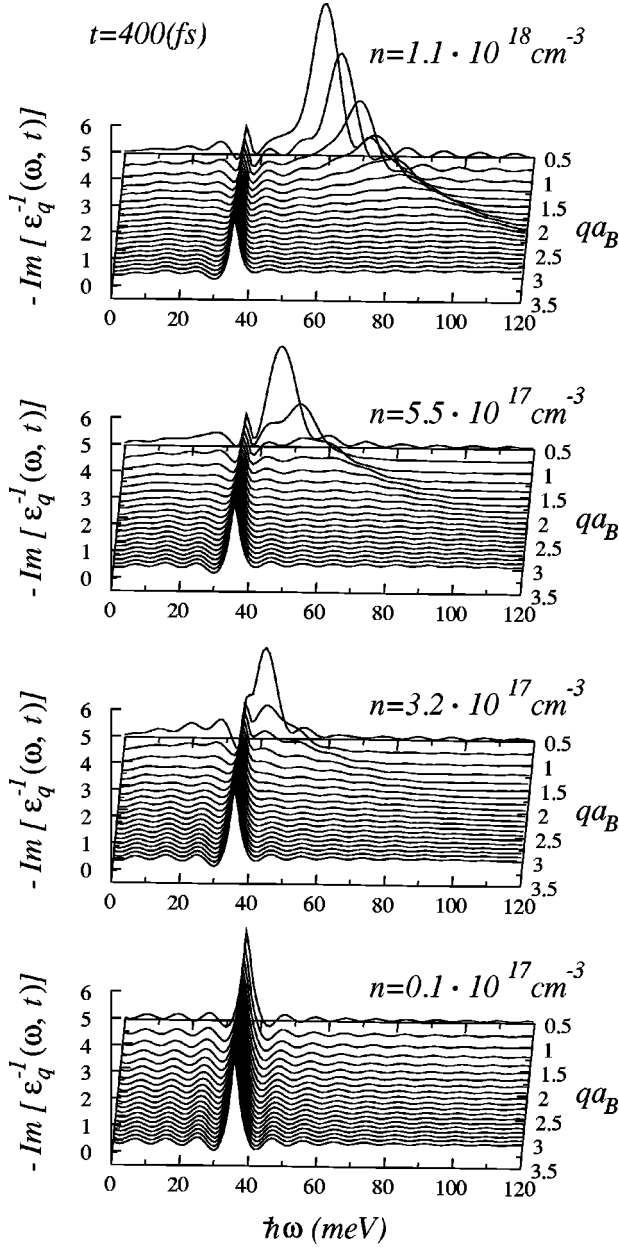


FIG. 4. Negative imaginary part of the inverse dielectric function versus frequency and wave number in units of the exciton Bohr radius a_B for the time $t = 400$ fs after an 11 fs pulse that excites the e - h densities $(0.1, 3.2, 5.5, 11) \times 10^{17}$ per cm^3 . The corresponding plasma frequencies are 5, 28, 36.5, 52.5 meV.

where E_g is the energy gap, $m_{e,h}$ are the effective masses of electrons and holes, respectively, and d is the interband dipole matrix element. The mean-field self-energy contains the Hartree-Fock exchange energy,

$$\Sigma_k^{MF}(t) = \begin{pmatrix} -\sum_q V_q \rho_{cc, \vec{k}-\vec{q}}(t) & -\sum_q V_q \rho_{cv, \vec{k}-\vec{q}}(t) \\ -\sum_q V_q \rho_{vc, \vec{k}-\vec{q}}(t) & -\sum_q V_q (\rho_{vv, \vec{k}-\vec{q}}(t) - 1) \end{pmatrix}, \quad (3.5)$$

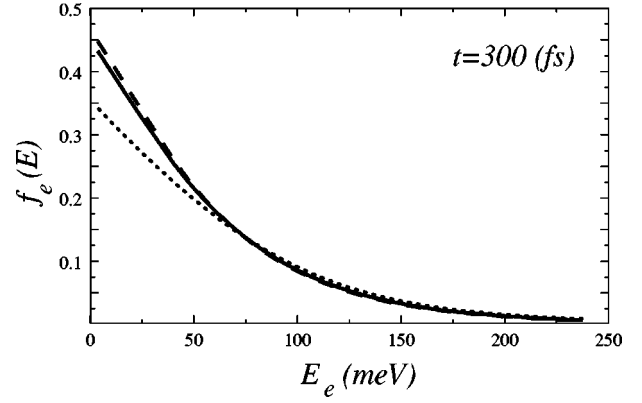


FIG. 5. Resulting electron distributions 300 fs after an 11 fs pulse that excited $n = 5.5 \times 10^{17} \text{ cm}^{-3}$ carriers in various approximations: scattering with screened LO-phonon-Coulomb interaction (full line), scattering with screened Coulomb interaction and unscreened phonon interaction (dashed line), and scattering with only screened Coulomb interaction (dotted line).

where the exchange energy with all electrons of the full valence band is subtracted, because it has been taken into account already in the band structure calculation.

The quantum kinetic scattering integrals are given by

$$\begin{aligned} \frac{\partial}{\partial t} \rho_{\vec{k}}(t)|_{scatt} = & -\frac{1}{\hbar} \int_{-\infty}^t dt' [\Sigma_{\vec{k}}^>(t, t') G_{\vec{k}}^<(t', t) \\ & - \Sigma_{\vec{k}}^<(t, t') G_{\vec{k}}^>(t', t) - G_{\vec{k}}^>(t, t') \Sigma_{\vec{k}}^<(t', t) \\ & + G_{\vec{k}}^<(t, t') \Sigma_{\vec{k}}^>(t', t)]. \end{aligned} \quad (3.6)$$

In the following we will present numerical results from the integration of this closed set of nonlinear integro-differential equations. We will assume a pulse with a width $\delta t = 11$ fs and a hyperbolic secant shape in the form $E(t) = [E_0 / \cosh(1.7627t / \delta t)] e^{-i\omega t}$. The frequency is detuned with respect to the band gap by $\hbar\omega - E_g = 50$ meV. The material parameters are those of GaAs and the phonon bath temperature is 300 K.

IV. THE TIME-DEPENDENT INVERSE DIELECTRIC FUNCTION

For a better understanding of the resulting effective interaction potential $W_q^r(t, t')$ we perform an incomplete Fourier transform over the earlier time t' ,

$$W_q^r(t, \omega) = \int_{-\infty}^t dt' W_q^r(t, t') e^{i\omega(t-t')}. \quad (4.1)$$

The complex dielectric function is then defined by

$$W_q^r(t, \omega) = \frac{V_q}{\epsilon_q(t, \omega)}. \quad (4.2)$$

In Fig. 2 we show the imaginary part of the inverse dielectric function versus wave number and frequency. The pulse strength is chosen to excite 1.1×10^{18} e - h pairs per cm^3 . For better visibility we plot $-\text{Im}(1/\epsilon)$ for various

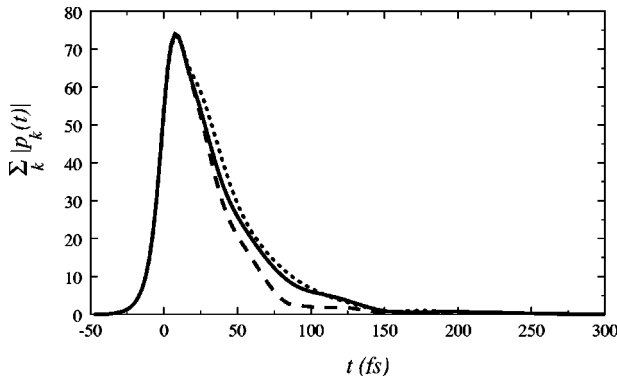


FIG. 6. Resulting incoherently summed interband polarization $\sum_k |p_k(t)|$ versus time after an 11 fs pulse centered at $t=0$ that excited $n=5.5 \times 10^{17} \text{ cm}^{-3}$ carriers in various approximations: scattering with screened LO-phonon-Coulomb interaction (full line), scattering screened Coulomb interaction and with unscreened phonon interaction (dashed line), and scattering with only screened Coulomb interaction (dotted line).

times after the pulse. One sees clearly the sharp resonance of the dispersionless LO phonon with an energy of 36 meV and the buildup of the plasmon resonance with a higher frequency of $\hbar \omega_{pl} = 52.5 \text{ meV}$. Its quadratic wave number dependence $\approx \omega_{pl}(1 + \frac{1}{2}q^2/\kappa^2)$, where κ is an inverse screening length, is seen from the projection of the maxima of the plasmon resonance into the ω - q plane.

At 50 fs the phonon resonance is sharp while the plasmon resonance is very broad because the buildup of screening is only in its early phase. At 400 fs the stationary resonance structure is essentially reached. One sees that at small wave numbers most of the oscillator strength of the LO phonon is transferred to the plasmon. On the other hand the plasmon amplitude falls off rapidly for larger momentum transfer, while the phonon amplitude is seen to increase with increasing q values. In Fig. 3 spectra of the negative imaginary part of the inverse dielectric function are shown for a lower density of excited carriers, namely, for $n=5.5 \times 10^{17} \text{ cm}^{-3}$, where the plasma frequency with $\hbar \omega_{pl} = 36.5 \text{ meV}$ is nearly degenerate with the $\hbar \omega_0 = 36 \text{ meV}$ LO-phonon frequency. In comparison with Fig. 3 one sees that the phonon has gained weight. This trend in the transfer of oscillator strength from the plasmon to the phonon with decreasing density is very clearly seen in Fig. 4 where we compare at later time ($t=400 \text{ fs}$) four spectra with densities ranging from 1.1×10^{18} to $0.1 \times 10^{17} \text{ cm}^{-3}$. At the lowest density the oscilla-

tor strength of the plasmon pole that lies on the low-energy side of the phonon pole is transferred completely to the phonon. This fact explains why one sees in time-integrated femtosecond four-wave mixing with coherent control only oscillations due to the upper branch of the mixed phonon-plasmon mode, i.e., phonon oscillations at low densities and plasmon oscillations at high densities, because small wave number transfer dominates the dephasing scattering.^{13,14}

Finally, in Figs. 5 and Fig. 6, we compare the resulting relaxation and dephasing kinetics for three approximations: one with the discussed combined effective screened LO-phonon-plasmon interaction (full lines), one with screening of the Coulomb interaction but unscreened phonon interaction (dashed lines), and finally one in which only the screened Coulomb carrier-carrier interaction is taken into account. In the relaxation of the electron distribution (see Fig. 5), one sees that the carriers relax faster to the low-energy states if the phonon scattering is also taken into account. Screening of the phonon interaction (in addition to that of the Coulomb interaction) makes the relaxation slightly slower in comparison with the model of unscreened LO-phonon scattering. Figure 6 shows correspondingly the same expected trends in the dephasing of the optically induced interband polarization: The contribution of phonon scattering in addition to the screened Coulomb scattering makes the dephasing faster, while screening also of the phonon interaction reduces its influence again in comparison with unscreened phonon scattering.

In conclusion, we have presented a self-consistent calculation of the combined screening of the carrier interactions via LO phonons and via the Coulomb potential in nonequilibrium electron systems, by making use of the Langreth theorem. The time dependence of the formation of the screened LO-phonon-plasmon pole structure of the effective interaction has been calculated and discussed. We showed that the oscillator strength at small momentum transfer is always concentrated at the resonance of the upper branch of the mixed modes. The influence of the screening of both the LO-phonon mediated interaction and the Coulomb interaction on the relaxation and dephasing kinetics after a short femtosecond pulse has been shown.

ACKNOWLEDGMENTS

We appreciate helpful discussions with P. Gartner and L. Bányai, and the fruitful cooperation with M. Wegener. This work was supported by the DFG-Schwerpunktprogramm ‘‘Quantenkohärenz in Halbleitern.’’

¹G.D. Mahan, *Many-Particle Physics* (Plenum, New York, 1981).

²J. Shah, *Ultrafast Spectroscopy of Semiconductors and Semiconductor Microstructures* (Springer, Berlin, 1996).

³H. Haug and A.P. Jauho, *Quantum Kinetics in Transport and Optics of Semiconductors* (Springer, Berlin, 1996).

⁴L. Bányai, Q.T. Vu, B. Mieck, and H. Haug, *Phys. Rev. Lett.* **81**, 882 (1998).

⁵P. Lipavský, V. Špička, and B. Velický, *Phys. Rev. B* **34**, 6933 (1986).

⁶L.V. Keldysh, *Zh. Éksp. Teor. Fiz.* **47**, 1515 (1964) [*Sov. Phys. JETP* **20**, 1018 (1965)].

⁷D.C. Langreth, in *Linear and Nonlinear Electron Transport in Solids*, edited by J.T. Devreese and E. van Doren (Plenum, New York, 1976).

⁸P. Gartner, L. Bányai, and H. Haug, *Phys. Rev. B* **60**, 14 234 (1999).

⁹D.B. Tran Thoai, L. Bányai, E. Reitsamer, and H. Haug, *Phys. Status Solidi B* **188**, 387 (1995).

¹⁰H. Haug and L. Bányai, *Solid State Commun.* **100**, 303 (1996).

¹¹L. Bányai, H. Haug, and P. Gartner, *Eur. Phys. J. B* **1**, 209 (1998).

¹²A. Baltuska, Z. Wei, M.S. Pshenichnikov, D.A. Wiersma, and R. Szipöcs, *Appl. Phys. B: Lasers Opt.* **65**, 175 (1997).

¹³M.U. Wehner, M.H. Ulm, D.S. Chemla, and M. Wegener, *Phys. Rev. Lett.* **80**, 1992 (1998).

¹⁴Q. T. Vu, H. Haug, W. A. Hügel, S. Chatterjee, and M. Wegener, preprint.